

See discussions, stats, and author profiles for this publication at: <https://www.researchgate.net/publication/344653510>

ON THE SOLUTION OF BLOOD FLOW MODEL USING BESSEL FUNCTION

Thesis · October 2020

DOI: 10.13140/RG.2.2.35161.13925

CITATIONS

0

READS

447

1 author:



[Ekle Ocheme Anthony](#)

Moscow Institute of Physics and Technology

1 PUBLICATION 0 CITATIONS

SEE PROFILE

**ON THE SOLUTION OF BLOOD FLOW MODEL USING BESSEL
FUNCTION**

BY

EKLE ANTHONY OCHEME

14/29788/UE

**A PROJECT WORK SUBMITTED TO THE DEPARTMENT OF
MATHEMATICS/STATISTICS/COMPUTER SCIENCE, UNIVERSITY OF
AGRICULTURE, MAKURDI IN PARTIAL FULFILMENT OF THE
REQUIREMENTS FOR THE AWARD OF A BACHELOR OF SCIENCE
(B.Sc) DEGREE IN MATHEMATICS/COMPUTER SCIENCE**

APRIL, 2018

DECLARATION

I hereby declare that this research work represents my original work and has not been previously submitted for the award of any degree in any university or similar institution.

NAME OF CANDIDATE: EKLE ANTHONY OCHEME

SIGNATURE OF CANDIDATE: 

DATE: 17/05/2018

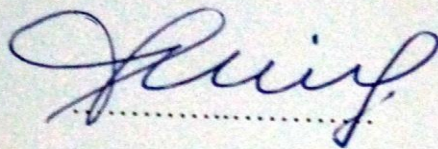
CERTIFICATION

We the undersigned, hereby certify that this project work by EKLE ANTHONY OCHENE with registration number 14/29788/UE meets the requirement for the award of the degree of Bachelor of Science in Mathematics/Computer Science (B.Sc Mathematics/Computer Science).

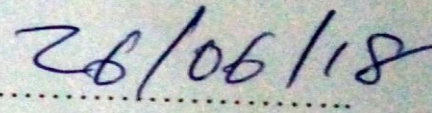
Title of Project: On the Solution of Blood Flow Model Using Bessel Function

Dr. T. Tivde

Project Supervisor



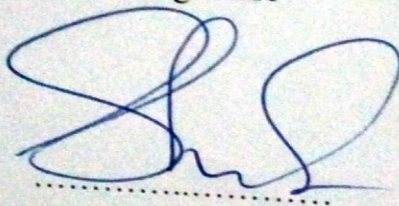
Signature



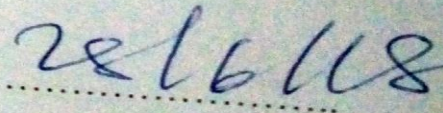
Date

Dr. S. C. Nwaosu

Head of Department



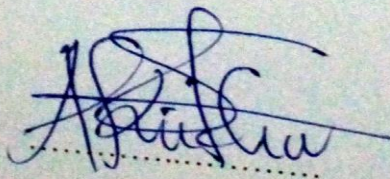
Signature



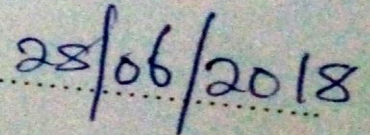
Date

Dr. B. G. Akuchu

External Examiner



Signature



Date

DEDICATION

This project work is dedicated to God Almighty, who in His faithfulness and loving kindness has embedded in me the mighty strength which was fully utilized at the course of this work; and most especially for making this research work a success. To my lovely mother Mrs. Ekle Patricia and to my late father Mr. Ekle Benedict.

ACKNOWLEDGEMENT

In a special way, I wish to sincerely express my heart gratitude to God Almighty for His mercy and wonderful works upon my life and in particular, for this project work.

My honest appreciation goes to my supervisor; Dr. T. Tivde, he has been more than a tutor to me, in fact he has been a father and I will never forget your words of encouragement. I want to also say a big thank you, because despite your tight schedules and busy times you were always there for me; may God reward you richly sir.

I want to say a big thank you to the HOD and all the lecturers and staff in the Department of Mathematics Statistics Computer Science for their support and selfless contribution to my academics in one way or the other. Indeed, I cherish and admire your wealth of knowledge, may the Lord almighty bless you all.

I wish to appreciate my lovely mother, Mrs Ekle Patricia for all her sacrifice of love and most of all for never giving up on me in spite of the conditions she had been through. I remain indebted to you ma'am; may God almighty preserve you and keep you save.

In addition, I wish to express my gratitude to all my family members, must especially my siblings (Mrs Ojor Grace, Ekle Blessing, Ekle James, Ekle Peter and Ekle Emmanuel). I appreciate your love, prayers and supports in my academic pursuit, May the good Lord in his infinite mercy bless you all.

I sincerely appreciate all my course mates and friends especially: Ogwuche Jeremiah, Adakole Prosper, Ameh Anthony, Angwue Sewese Dorcas, Verkyav Peter and James Johnson for their encouragement and maximum support all through my stay in school.

Finally, I cannot forget to say a big thank you to the family of Barrister Olatunde and Dr (Mrs) Helen Olatunde for being so kind and caring to me. Ma'am; indeed, you have being a mother to me all through my stay in school, only God almighty can reward you.

ABSTRACT

The research involves an analytical examination of Navier-Stokes equation concerning the unsteady-state laminar flow of an incompressible (Newtonian) fluid in an infinitely long horizontal circular pipe spinning about its symmetry axis, say z , and inside which the liquid motion starts with an axial velocity component as well. Basic physical assumptions are that the pressure axial gradient keeps itself on its hydrostatic value and that no radial velocity exists. In such a way the Navier-Stokes PDEs become uncoupled and can be faced separately. We succeed in computing the unsteady speed components along the axial direction by means of Bessel function and its properties, in which we obtained the exact solution using MATLAB. Following this, we obtained the velocity profile that describes the flow rate alongside the shear stress at the wall and we observed that the velocity and shear stress profile provides an accurate analysis with small time duration that includes impulse loads such as oscillation flow of blood in an artery.

TABLE OF CONTENT

Title Page

i

Declaration	ii
Certification	iii
Dedication	iv
Acknowledgement	v
Abstract	vii
Table of Content	viii
CHAPTER ONE	1
INTRODUCTION	1
Background of Study	1
Statement of Problem	3
Aim/Objective of Study	3
Significance of Study	4
Scope of Study	5
Definition of Terms	5
CHAPTER TWO	10
LITERATURE REVIEW	10
Historical Background	10
Review of the Womersley Arterial Flow	12
The One-Dimensional Model of Blood Flow in the Mesenteric Arterial Sys.	15

The Contemporary Solutions of the Navier-Stokes	17
Summary of the Review	19
CHAPTER THREE	21
RESEARCH METHODOLOGY	21
Model Formulation	21
Governing Equations	22
Momentum equations for incompressible flow in a cylindrical coord.	22
Axial Momentum Equation	23
3.3 Solution to the Axial Navier-Stokes	24
3.4 The Method of Separation of Variables	25
3.5 Solution of the Bessel Differential Equation	28
3.6 Axial Velocity through the Pipe	31
3.7 Orthogonality of the Bessel Function	33
3.8 Shear Stress Distribution in the Pipe	34
CHAPTER FOUR	36
RESULT, DISCUSSION AND CONCLUSION	36
4.0 Introduction	36

4.1	Results	36
4.2	Discussion	45
4.2.1	Discussion on the Axial Velocity Profile Graph in Figure 4.4	45
4.2.2	Discussion on the Shear Stress Distribution Graph in Figure 4.7	46
	Conclusion	47
	REFERENCES	48

CHAPTER ONE

INTRODUCTION

1.1 Background of Study

Mathematical modeling of blood flow has attracted wide attention since the discovery of blood circulation in 1628 by William Harvey and the discovery of the capillaries by Marcello Malpighi in 1675 using microscope. (Walker, 1958)

Blood being the major component of our body system, it is a concentrated suspension of several forms of cellular elements; red blood cells (RBCs or erythrocytes), white blood cells (WBCs or leukocytes) and platelets in an

aqueous polymeric and ionic solution, the plasma, large quantity of water and other organic compounds. Hence, making the whole blood complex mechanical properties, in this case; blood cannot be modeled as a homogenous fluid and it is essential to consider it as a suspension of blood cells in plasma (especially RBCs). As the consequences of this behaviour; blood is seen as an unsteady flow, non-uniform and an incompressible fluid. The whole blood has complex mechanical properties, which depends mainly on the size of the blood vessels and the flow behavior. Hence, it is approximated as a Navier-Stokes equation or a Non-Newtonian fluid. Despite the important works done on this equation, our understanding on them remains fundamentally incomplete, due to their nature of nonlinearity.

Since the introduction of the one-dimensional modeling of the human arterial system by Euler (1775), many blood flow models have evolved; some reviewed in this study. But single model which can fully capture all aspect of the hemodynamic of the human arterial system is yet to be developed. Great attempt was made by Womersley (1955); he applied mathematical and computational techniques to the analysis of blood flow, characterizing it as an unsteady flow. In recent years a few three-dimensional models have been developed, including the three-dimensional numerical models by Perktold *et al*, (1991) to study the Pulsatile flow field and the effect of wall shear stresses on the development of lesions. In the early twentieth century G. M. Atlas and M. C. Desilverio did a work on a model of Aortic Blood flow, in which a quantitative modeling of large arteries was used to predict and describe functional hemodynamic component of blood flow (Atlas & Desilverio; 2006). The same year (Marmanie *et al*, 2006) worked on a one-dimensional model of

the Navier-Stokes of a nonlinear dynamical system which was analysed as a simplified model of the dynamics ensued by the NS equation.

In 2009 a unique approach was made where investigation on the Critical thresholds in a quasi-linear hyperbolic model of blood flow with viscous damping was investigated, using the invariant Riemann integral (Tong, 2009). The most recent of all is the work done by G. Brenn titled: “Analytical Solutions for Transport Processes”, in which he considered a spatially two-dimensional linear unsteady flow, with the flow velocity varying with the coordinate y , but not with x (Brenn, 2017).

Therefore, in this study we shall focus more on the solution of the three-dimensional unsteady form of the Navier-Stokes (NS) equations, using the Bessel special functions, the functions which are canonical solutions of the Bessel differential equations. The Bessel functions defined by Daniel Bernoulli and generalized by Friedrich Bessel; is one of the varieties of special functions which are encountered in the solution of physical problems. The NS equations were derived independently by George Gabriel Stokes, in England, and Claude-Louis Navier, in France, in the early 1800's. The equations are extensions of the Euler Equations and include the effects of viscosity on the flow. These equations are very complex, yet solvable.

1.2 Statement of Problem

Blood flow models are governed by partial differential equations. Many approaches have been made to solve such blood flow models. These approaches as well as methods among many others include numerical methods

like; Finite difference method, finite element methods, transforms methods, Laplace, Fourier and Hankel Transforms methods.

In this project, we use the Bessel function in obtaining the solution of blood flow models under consideration.

1.3 Aims and Objectives of Study

The aim of this project is to study the solution of blood flow models via the Bessel special function.

The study is set specifically to:

- i. identify the Navier-stokes equation and the momentum equations for incompressible flow in cylindrical coordinates from literatures.
- ii. generate the axial momentum equation governing the fluid flow.
- iii. find the solutions of the axial momentum equations and also the independent solutions of the Bessel differential equations.
- iv. obtain the velocity profile that describes the characteristic of the incompressible fluid flow and the shear stress at the wall.

1.4 Significance of Study

The significance of this study is to improve more on the approximate simulation of the Blood flow model which is exceptionally hard to find a good approximation, even with supercomputers. This solution reviews essential characteristics of the blood flow which in turn will help physicians to make effective medical treatment, planning and development of predictive blood

related diseases. The study of shear stress also help medical experts in regulating the inflammatory processes that initiate and enhance the growth of the fibro inflammatory lipid plaque that grows in the wall of the womb.

In as much as the solutions of Navier-Stokes equation contributes greatly to the medical field, studying of the non-Newtonian fluid (i.e. Rheology), has great application in material science, engineering, geophysics, human biology and even pharmaceuticals. This research work will contribute greatly to major commercial industries in Nigeria, Africa and the world at large to improve quality of products. Companies like cement, paints, plastics and chocolate which have complex flow characteristics. The pharmacists, as well, not left out; the study of flow properties of liquid like blood helps in the manufacture of several forms. Such as ointments, creams, pastes etc. Notwithstanding, for a country like Nigeria, government agencies can use the study of flow properties as important quality control tools to maintain the superiority of products and reduce batch to batch variations; which will contribute to developing firms.

In addition, most problems where the Navier-Stokes equations apply include other multi-physical phenomena. For example: Aero-elastic problems with compressible flow, combustion chemistry in flow fields. In such a case, solving the Navier-Stokes equations with special functions like the “Bessel” gets us part of the solutions. Another interesting contribution of this study is that if we could establish solvability of the Navier-Stokes, we could as well develop methods that were more efficient in solving these problems. For example: the Large Eddy Simulation which uses the properties of Navier-Stokes equations to compute fluid profiles.

1.5 Scope of Study

The research work is limited to studying the unsteady state laminar flow of an incompressible fluid in a cylindrical pipe spinning about its symmetry axis, say z . To this end, we obtain the axial velocity profile and the shear stress at the wall; by the means of the Bessel special function, its properties and infinite series expansion of Forurier-Bessel type under time exponential damping.

1.6 Definition of Terms

1.6.1 Bessel Equation:

The Bessel equation is a linear second order Ordinary Differential Equation of type:

$$x^2 y'' + xy' + (x^2 + v^2)y = 0$$

Where the number v is called the order of the Bessel equation, the DE is named after the German mathematician and an Astronomer Friedrich Wilhelm Bessel who studied the equation in detail and show that its solutions are expressed in terms of a special class of functions called cylindrical functions or Bessel functions.

1.6.2 Bessel Function of the First Kind ($J_{n(x)}$):

The Bessel function of the first kind denoted by $J_{n(x)}$, are defined as the solutions to the Bessel equation which are finite at the origin ($x = 0$) for integer or positive n and diverges as x approaches zero for negative non-integer (n).

$$J_{n(x)} = \sum_{k=0}^{\infty} \frac{(-1)^k}{k! \Gamma(n+k+1)} \left(\frac{x}{2}\right)^{2k+n}$$

or

$$J_{-n}(x) = \sum_{k=0}^k \frac{(-1)^k}{k! \Gamma(k - n + 1)} \left(\frac{x}{2}\right)^{2k-n}$$

1.6.3 Newtonian and Non-Newtonian Fluids:

A Newtonian fluid is a fluid with constant viscosity, no matter the amount of shear force applied for a constant temperature. For example: water, mineral oil, gasoline, alcohol etc. these fluids have a linear relationship between viscosity and shear stress.

While, Non-Newtonian fluids are opposite of Newtonian fluids, shear forces are applied to non-Newtonian fluids, the viscosity of the fluids changes.

1.6.4 Steady and Unsteady Flow:

A steady flow is one in which all conditions at any point in a stream remain constant with respect to time, for example; laminar flow (i.e. viscous liquid), while; unsteady flow is referred to a flow in which quantity of liquid flowing per second is not constant. When a valve is closed at the discharge end of the pipeline causing velocity and pressure to fluctuate within the pipe

1.6.5 Uniform and Non-Uniform Flow:

A uniform flow is one in which velocity is the same at a given instant at every point in the fluid. While, in non-uniform flow, velocity is not constant at a given instant of time.

1.6.6 Navier-Stokes Equation:

The Navier-Stokes equation is named after Claude-Louis Navier and George Gabriel Stokes; it describes the motion of viscous fluid substances. These balance equation arise from applying Newton's second law to fluid motion, together with the shear stress force in the fluid. These equations describe how the velocity, pressure, temperature, and density of a moving fluid are related.

$$\begin{array}{c}
 \text{Inertial (per volume)} \qquad \qquad \qquad \text{Divergence of stress} \\
 \rho \left(\underbrace{\frac{\partial v}{\partial t}}_{\text{Eulerian acceleration}} + \underbrace{v \nabla v}_{\text{Advection}} \right) = \underbrace{-\nabla P}_{\text{Pressure gradient}} + \underbrace{\mu \nabla^2 v}_{\text{Viscosity}} + \underbrace{f}_{\text{Other body force velocity}}
 \end{array}$$

Where:

v = Velocity for the fluid parcel or axial velocity

μ = Kinematic Viscosity

P = Pressure

ρ = Fluid density

∇ = Divergence

1.6.7 Shear Stress Force:

These are forces in a fluid tending to cause deformation of the container. It arise from shear forces, which are pairs of equal and opposite forces acting on opposite sides of an object, represented by a Greek letter “ τ ” given by

$$\tau = \frac{F}{A} = \frac{\text{Force Applied}}{\text{Cross-Sectional Area Of Material}}$$

1.6.8 Computational Fluid Dynamics:

This is a field of fluid mechanics that uses numerical analysis and data structure to solve and analyze problems that involve fluid flow.

Computational fluid dynamics (CFD) is the field of Applied Mathematics, Physics and computational software to visualize how a gas or liquid flows, as well as how the gas or liquid affects objects as it flows past. Computational fluid dynamics is based on the Navier-Stokes equations.

1.6.9 Large Eddy Simulation (LES):

The Large Eddy Simulation is a mathematical model for turbulence (i.e. a flow in fluid dynamics characterized by chaotic changes in pressure and flow velocity) used in computational fluid dynamics.

1.6.10 Frobenius method:

In Mathematics, the Method of Frobenius, named after Ferdinand Georg Frobenius, is a way to find an infinite series solution for a second-order ordinary differential equation of the form:

$$x^2u'' + P(x)xu' + Q(x)u = 0, \text{ in the vicinity of the regular singular point.}$$

1.6.11 Axial Velocity profile:

In fluid dynamics, axial velocity simply means the velocity in the axial plane (i.e. the z-axis) in a three-dimensional coordinate system. The velocity profile not only shows you the magnitude of velocity in the fluid, but also shows you the characteristics of the flow like direction, change due to shape of the domain or increase/decrease in the velocity magnitude with respect to the

geometry. Generally, it helps you to understand how the fluid behaves while it is transported through the domain.

1.6.12 viscosity:

Viscosity is basically a measure of the fluid's resistance to motion. It is a property of the fluid. Viscous effects are caused by the shear stress between a fluid and the wall of a pipe.

CHAPTER TWO

LITERATURE REVIEW

2.1 Historical Background

It is almost 1500 years that most of the society followed Galenic teachings involving the circulation of the blood throughout the body, which were a logical evolution from the teachings of Aristotle and other Greeks. Galen (c. AD 130-200) in the early 160s AD viewed the cardiovascular system as comprising two distinct networks of arteries and veins. Galen claimed that the liver produced blood that was then distributed to the body in a centrifugal manner, whereas Blood was not seen to circulate but rather to slowly ebb and flow. This view hold way for 15 centuries until the discovery made by

Harvey(1628) in his major work, “De Motu Cordis” (“On the Motion of the Heart and Blood”) Harvey employed experiment and deductive logic to show that arteries and veins are functional and that blood circulates round the body system. But, before this discovery Andreas Vesalius (1514-1564) discovered an illustration concerning human anatomy. He found that the blood vessels came from the heart and not the liver as Galen had earlier believed. In his work, “De Humani Corporis Fabrica”, he carefully, but strongly, questioned Galen’s views, which were taught in the schools of medicine during his time (Garber, 2010; Michael, 2011).

Modeling of blood flow has attracted wide attention since the discovery of blood circulation in 1628 by William Harvey and the discovery of the capillaries by Marcello (1675). The motion of the fluid is considered as the rate of change of momentum of an element of fluid and the forces on it, as proposed by Newton’s second law for particles. Newton himself did not explain well the nature of the forces between the particles in a continuum, but started the dynamics of a viscous fluid in an intuitive form (Principia, 1687). The law which is represented as:

$$F = ma \tag{1}$$

After Newton, the second law was applied by Euler (1750) to continuum mechanics, leading up to the publication in 1757. In this, he provided the system ruling a frictionless fluid motion, compressible or not, under an arbitrary set of external forces. He worked on one-dimensional modeling of the human arterial system, while his predecessors had worked on incompressible ones with one-dimension (Bernoulli and Bernoulli) or two-dimension (D’Alembert) degrees of freedom. But the birth of the Navier-

Stokes equations came much later: it is linked to the birth of elasticity theory which, at the beginning of the 19th century, was an important asset to engineers looking for a sound theory of the beam bending. Navier (1827) extended his previous theory to hydrodynamics and this led him to a new internal force in Euler's equations: a new μ -force which was generated by the non-uniformity of the motion of the fluid. Many years later, the Navier-Stokes equations, as we now know them, were deduced from various physical hypotheses, for instance the stress linearly related to the strain rate of the fluid, by Stokes (1849), who clearly reviewed the methods and hypotheses of Navier and other authors, presented a short rational approach to the equations of viscous fluids. Stokes proposed that fluids are classified on the rate at which they deform in response to an imposed shear stress: in Newtonian fluids there is a linear relation between the shear stress and the strain rate, whereas in Non-Newtonian ones this relation is non-linear. The Navier-Stokes equations rule the motion of fluids in general, and are applicable to Newtonian as well as Non-Newtonian fluids, to both laminar and turbulent flows of liquid/gas.

Since the introduction of the one-dimensional modelling of the human arterial system by Euler (1775), many blood flow models have evolved with unique solution approaches including methods like; Finite difference method, finite element methods, transforms methods, Laplace-Fourier and Hankel Transforms methods, but a single model which can fully capture all aspects of the hemodynamic of the human arterial system is yet to be developed.

2.2 Review of the Womersley Arterial Flow

In fluid dynamics, a flow with periodic variations is known as pulsatile flow, or as Womersley flow. The flow profile was first derived by Womersley

(1907–1958) in his work with blood flow in arteries titled: “Method for the Calculation of Velocity, Rate of Flow and Viscous Drag in Arteries When the Pressure Gradient Is Known”.

Womersley's model makes use of Poiseuille flow, and is a simplification of the Navier-Stokes equations. The work evolved from the experiments of McDonald and his co-workers (McDonald, 1952, 1955; Helps & McDonald, 1953) have shown that in the larger arteries of the rabbit and the dog there is a reversal of the flow. Measurements of the pressure gradient (Helps & McDonald, 1953) showed a phase-lag between pressure gradient and flow somewhat analogous with the phase-lag between voltage and current in a conductor carrying alternating current.

Womersley considered a circular pipe of length l , radius R , filled with a viscous liquid of density ρ and viscosity μ . The quantity $\nu = \mu/\rho$, as the kinematic viscosity. To clarify what is to follow, he compared the solution at each stage with the corresponding well-known Poiseuille solution for steady flow. In steady flow, he stated that: if P_1 and P_2 are the pressures at the ends of the pipe, the constant pressure gradient throughout a pipe of length l given as:

$$\frac{P_1 - P_2}{l} \quad (2)$$

A Poiseuille flow assumes that the flow is steady, uniform (over a cross-section), laminar, and axially symmetric within a cylindrical tube. Under these assumptions, the term:

$$\frac{\partial \omega}{\partial t} = 0$$

Since there is no change in velocity over time, furthermore, the terms $\frac{\partial \omega}{\partial x}$ and $\frac{\partial \omega}{\partial \theta}$ equal zero. (Womersley, 1955)

After accounting for the simplifications of the Navier-Stokes equations based on Poiseuille flow, the Poiseuille flow along with the velocity of the fluid was described by the following equation.

$$\frac{d^2 \omega}{dr^2} + \frac{1}{r} \frac{d\omega}{dr} + \frac{p_1 - p_2}{\mu l} = 0 \quad (3)$$

Womersley went further to express the pressure gradient as a periodic function of time with frequency $f = \frac{n}{2\pi}$ to represent the arterial pulse. Solving for flow velocity, and resolving the above equation in Bessel form; Womersley's arterial flow model gives formulas to calculate the flow rate of a viscous fluid through a rigid tube under a periodic pressure gradient, described by a Fourier series. The solution is then extended to calculate the flow rate over a cross-sectional area of the tube. Womersley's number has provided both fluid mechanics and biological sciences with a means to measure the inertial forces versus the viscous forces. It is as significant in analyzing unsteady flow as the Reynolds number is in measuring steady flow. Womersley's model has been foundational to many models of arterial blood flow, but it is limited to modeling laminar flow through a rigid, cylindrical tube. In reality, there are elastic effects in the blood vessel and the pressure gradient may depend on other factors besides time. In addition, Womersley's model considers only longitudinal velocity, whereas there may also be a radial part (Womersley, 1955).

More studies and effective application of the Womersley Arterial flow have been developed in the last decades; including the research of (David *et al.*, 2002) “Arterial Wall Properties and Womersley Flow in Fabry Disease”. The authors were able to examine the mechanical properties of the radial artery in Fabry disease, a typical fibro-muscular artery. Real time B-mode ultrasound recordings of the right radial artery were obtained simultaneously allowing calculation of the vessel wall internal and external diameter, the incremental Young's modulus and arterial wall thickness. By simultaneous measurement of the distal index finger-pulse oximetry the pulse wave speed was calculated. From the wave speed and the internal radial artery diameter the volume flow was calculated by Womersley analysis following truncation of the late diastolic phase. Also in a journal titled “Computer methods and programs in Biomedicine” collective authors worked on the Womersley number-based estimation of flow rate with Doppler ultrasound: Sensitivity analysis and first clinical application. The authors continue in their investigation proposed in a paper recently published, for a reliable estimation of (peak systolic) blood flow rate from velocity Doppler measurements, more insight was given on the sensitivity analysis of the formulas relating blood flow rate to velocity. In particular the authors’ analyze how our estimates are affected by perturbation or errors in measurements in comparison with a standard method for catheter based estimates based on the assumption of a parabolic velocity profile (Vergara *et al.*, 2009).

2.3 The One-Dimensional Model of Blood Flow in the Mesenteric Arterial System

The model of blood flow in the mesenteric arterial system is a collective research carried out by Mabotuwana, Leo and Andrew (2007) aimed at developing an extensible anatomically and biophysically based computational model of the mesenteric arterial system, which is the main blood supply to the human intestine, and the model was used to carefully examine the intestinal blood flow. The authors' were able to treat the blood flow within the mesenteric system as one-dimensional and solve this model using numerical techniques developed previously by Smith *et al* (2001) in which, an efficient provision of the numerical scheme to model pulsatile three-dimensional blood flow using a single dimension, and simulate vessel diameter changes and pressure distributions was made.

In the study, blood was assumed to be Newtonian fluid a common assumption in blood flow analysis in large to medium sized vessels. Since a typical Reynolds number in the abdominal aorta is around 590 and this is well below the critical Reynolds number (which is generally considered to be 2300) above which the transition from laminar to turbulent flow usually occurs, therefore laminar flow was assumed throughout the study. Furthermore, the authors' considered blood to be an incompressible, homogeneous fluid with an axisymmetric flow and constant viscosity. Under these assumptions, using a cylindrical coordinate system (r, θ, x) where the x axis is aligned with the local vessel axial direction and assuming a zero velocity in the circumferential direction, the complete 3-dimensional Navier-Stokes equations was gradually reduced to a set of 1-dimensional flow equations:

$$\frac{\partial R}{\partial t} + V \frac{\partial R}{\partial x} + \frac{R}{2} \frac{\partial V}{\partial x} = 0 \quad (4)$$

$$\text{And} \quad \frac{\partial V}{\partial t} + 2(1 - \alpha) \frac{V}{R} \frac{\partial R}{\partial t} + \alpha V \frac{\partial V}{\partial x} + \frac{1}{\rho} \frac{\partial P}{\partial x} = \frac{2v}{R} \left[\frac{\partial v_x}{\partial r} \right]_R \quad (5)$$

Where p , R , V , ρ and v represent: pressure, inner vessel radius, average velocity, blood density and blood viscosity respectively. The parameter α is used to specify the shape of the axial velocity profile, with $\alpha = 1$ corresponding to a flat profile.

By specifying an axial velocity profile in the x direction(v_x), the right hand side of (5) was solved to be:

$$v_x = \frac{\alpha}{2-\alpha} \left[1 - \left(\frac{r}{R} \right)^{\frac{2-\alpha}{\alpha-1}} \right] \quad (6)$$

From the governing equations above, the velocity profile across the vessel was generated. But, the governing equations could not be solved analytically leading to the use of numerical techniques. The Two-Step-Lax-Wendroff finite difference method was selected as a suitable explicit scheme as it is second order accurate in both space and time while eliminating large numerical dissipations; numerical solutions for pressure, vessel radius and velocity for the entire mesenteric arterial network were analyzed.

The results of Mabotuwana, Leo and Andrew (2007) indicate, that the simulation is numerically stable thereby is conserving mass and momentum. The profiles also show that continuity of pressure is maintained across all bifurcations points. Nevertheless, the work had some major limitations: One of the main drawbacks of the current model is that it is based on images from the male Visible Human dataset which represent the geometry of a deceased person, and therefore some of the vessels have either collapsed or are difficult

to identify, another major drawback with the current model is its inability to create the capillary and venous networks. The mesenteric arterial system being a sensitive organ in the human system has drawn attention of medical experts and researchers. In 2015, Acosta Stefan published an article, titled “Mesenteric ischemia”, the author was able to investigate that Intestinal revascularization in patients with arterial occlusive and mesenteric ischemia, reduces bowel morbidity and mortality (Acosta, 2015).

2.4 The Contemporary Solutions of the Navier-Stokes

A few three-dimensional models have been developed in recent years to study the effects of wall shear stresses on the development of lesions and atherosclerosis in simple arterial networks, including the works by (Perktold, Resch, Peter 1991; Taylor, Hughes, Zarins and Ann, 1998) in which the authors analyzed the Navier-Stokes with the Finite element methods and the numerical approaches. Desiliderio, (2006) studied blood model and focused on the model of Aortic Blood flow, in which a quantitative modeling of large arteries was used to predict and describe functional hemodynamic component of blood flow. The same year (Marmanie *et al.*, 2006) worked on a one-dimensional model of the Navier-Stokes of a nonlinear dynamical system which was analyse as a simplified model of the dynamics ensued by the NS equation. In some cases the unsteady problem of the Navier-Stokes leads to some nonlinear ODE as in Shapiro's paper “An analytical solutions of the Navier-Stokes equations for unsteady backward stagnation-point flow with injection or suction” (Zamm & Angew, 2006); about an unsteady axisymmetric incompressible case with a decelerating backward stagnation-

point flow with uniform injection or suction from a porous boundary (plate). The author arrives at a third order nonlinear ODE which after some work is transformed into a tractable equation.

Since the NS has a broad application in material sciences and fluid dynamics different analytical approaches keeps evolving depending on the field of application, for instance the works of (Tanskiv 2005; Polyanin *et al*; 2009), Muriel; Dresden, (2011) which the authors calculate the time evolution of the one-particle distribution function by applying the time evolution equations.

The most recent of all is the work done by G. Brenn, (2017) titled: “Analytical Solutions for Transport Processes”, in which he investigated that the hydrodynamic problem is faced not directly through the velocity components but via the Stokes stream function PDE. The author collects some recent research papers. A first example is a spatially two-dimensional linear unsteady flow, with the flow velocity varying with the coordinate y , but not with x . Another case: flow fields along infinite structures without any geometrical elements with length scales, for instance along at plates, without an imprinted flow time scale. In every case, the form assumed for the velocity profile caused the nonlinear inertia terms in the Navier-Stokes equation either to vanish completely or to produce only a centrifugal force, easily balanced by a pressure gradient. It is then possible, or convenient, to perform a linearization. The exact solutions presented so far are by him called “degenerate”: the linearization for cylindrical flows is solved by the approach of Tomotika. That for spherical flows leads to an equation for which the same approach leads to the Legendre functions of the first and second kind.

2.5 Summary of the Review

To summarize; although, nowadays, computer techniques make the complete integration of the Navier-Stokes equations feasible, the accuracy of numerical results can be established only by comparison with an exact solutions. From literatures, especially recent works on 2-D and 3-D unsteady incompressible flows it is quite difficult to analyze the non-linear unsteady flow with the analytical approach, with the flow velocity varying with the x coordinate as in (Brenn, 2017), but in this research, using the Bessel approach to resolve the ODEs, proper evaluation of the system was made.

In addition the few solutions of 3-dimensional incompressible flow as in literature were mainly analyzed numerically. But, the numerical approach has great challenges to consider shear wall boundary conditions in the cylindrical objects, as it may involve arbitrary domains. But, using the principle of superposition and the orthogonal properties of the Bessel special function the shear stress distribution along the wall of the tube (blood vessels) where considered.

Therefore, this research is focus mainly on the study of internal, laminar unsteady motion in the axial direction (i.e. blood flow as an incompressible fluid). And the model which we solved using the Bessel function of the order zero.

CHAPTER THREE

RESEARCH METHODOLOGY

3.1 Model Formulation

The Navier-Stokes equations are the fundamental PDE that describes the flow of incompressible fluids; the equation which is derived from the Newton's second law of motion.

$$F = ma \quad (7)$$

LHS:

To describe the internal force in an incompressible fluid, we consider the viscous force, pressure force and the external body force as listed below:

i. $F_{viscous} = \mu \nabla^2 u$

ii. $F_{pressure} = -\nabla P$ (*Pressure gradient*)

iii. $F_{body} = f$ (*body force*)

where:

$$\nabla = \frac{\partial}{\partial x_1} + \frac{\partial}{\partial x_2} + \frac{\partial}{\partial x_3} + \dots + \frac{\partial}{\partial x_n} \quad \text{And} \quad \nabla^2 = \frac{\partial^2}{\partial x_1^2} + \frac{\partial^2}{\partial x_2^2} + \frac{\partial^2}{\partial x_3^2} + \dots + \frac{\partial^2}{\partial x_n^2}$$

Putting the forces together we have:

$$F = -\nabla P + \mu \nabla^2 u + f \quad (8)$$

RHS:

The right hand side (ma) of the Newton's law describes the mass and acceleration in the fluid.

ρ = Volumetric mass density of the fluid

The acceleration is given as: $\left(\frac{\partial u}{\partial t} + u \cdot \nabla \cdot u\right)$ i.e. the velocity change with time.

$$ma = \rho \left(\frac{\partial u}{\partial t} + u \cdot \nabla \cdot u\right) \quad (9)$$

Putting (8) and (9) in (7) to get:

$$\rho \left(\frac{\partial u}{\partial t} + u \cdot \nabla \cdot u\right) = -\nabla P + \mu \nabla^2 u + f \quad (10)$$

Where:

u = *Velocity*

μ = *Viscosity*

P = *Pressure*

Equation (10) is called the Navier-Stokes equations represented in a vector form.

3.2 Governing Equations

3.2.1 Momentum equations for incompressible flow in a cylindrical coordinate system

Considering a three-dimensional coordinate, equation (10) can be represented in (r, θ, z) then we have $(u = u_r, u_\theta, u_z)$ components:

R-component:

$$\rho \left[\frac{\partial u_r}{\partial t} + u_r \frac{\partial u_r}{\partial r} + \frac{u_\theta}{r} \frac{\partial u_r}{\partial \theta} - \frac{u_\theta^2}{r} + u_z \frac{\partial u_r}{\partial z} \right] = -\frac{\partial P}{\partial r} + P g_r + \mu \left[\frac{1}{r} \frac{\partial}{\partial r} \left(\frac{\partial u_r}{\partial r} \right) - \frac{u_r}{r^2} + \frac{1}{r^2} \frac{\partial^2 u_r}{\partial \theta^2} - \frac{2}{r^2} \frac{\partial u_\theta}{\partial \theta} + \frac{\partial^2 u_r}{\partial z^2} \right] \quad (11a)$$

θ -component:

$$\rho \left[\frac{\partial u_\theta}{\partial t} + u_r \frac{\partial u_\theta}{\partial r} + \frac{u_\theta}{r} \frac{\partial u_\theta}{\partial \theta} - \frac{u_r u_\theta}{r} + u_z \frac{\partial u_\theta}{\partial z} \right] = -\frac{1}{r} \frac{\partial P}{\partial \theta} + P g_\theta + \mu \left[\frac{\partial}{\partial r} \left(\frac{1}{r} \frac{\partial u_r}{\partial r} \right) + \frac{1}{r^2} \frac{\partial^2 u_\theta}{\partial \theta^2} + \frac{2}{r^2} \frac{\partial u_r}{\partial \theta} + \frac{\partial^2 u_\theta}{\partial z^2} \right] \quad (11b)$$

Z –Component:

$$\rho \left[\frac{\partial u_z}{\partial t} + u_r \frac{\partial u_z}{\partial r} + \frac{u_\theta}{r} \frac{\partial u_z}{\partial \theta} + u_z \frac{\partial u_z}{\partial z} \right] = -\frac{\partial P}{\partial z} + P g_z + \mu \left[\frac{1}{r} \frac{\partial}{\partial r} \left(r \frac{\partial u_z}{\partial r} \right) + \frac{1}{r^2} \frac{\partial^2 u_z}{\partial \theta^2} + \frac{\partial^2 u_z}{\partial z^2} \right] \quad (11c)$$

Hereinafter called radial (11a), circumferential (11b) and axial (11c) respectively

3.2.2 Axial Momentum Equation

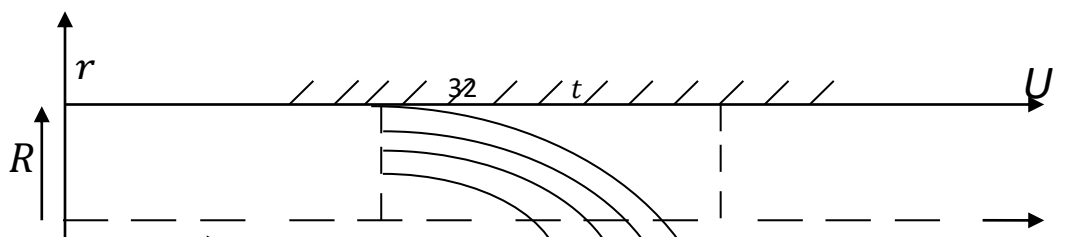


Figure 3.1: Fluid Movement induced in the Axial Direction.

To obtain the axial momentum haven considered an infinitely long horizontal circular pipe some basic assumptions are made:

- i. For the condition of the present unsteady parallel flows in the absence of body forces.
- ii. The permeable wall boundary is treated as fluid medium.
- iii. Setting the non-vertical components of gravity to zero and the vertical one to $-g$, that is, the velocity radial component is always zero, $u_r = 0$ for any r, θ, z, t thus:

$$U = (0, 0, u_z(r, t)). \quad (11d)$$

In such a case the circumferential (11b) and axial (11c) equations of the Navier-Stoke system become uncoupled, so that they can be treated separately.

Hence, the axial velocity is the only nonzero velocity component.

The axial momentum equation is reduced to:

$$\rho \frac{\partial u_z}{\partial t} = \mu \left[\frac{1}{r} \frac{\partial}{\partial r} \left(r \frac{\partial u_z}{\partial r} \right) + \frac{1}{r^2} \frac{\partial^2 u_z}{\partial \theta^2} \right] \quad (12)$$

Since the flow is rotationally symmetric (i.e. the same after series of rotation), equation (12) is further reduced to:

$$\frac{\partial u_z}{\partial t} = \frac{\nu}{r} \frac{\partial}{\partial r} \left(r \frac{\partial u_z}{\partial r} \right) \quad (13)$$

Where: $\nu = \frac{\mu}{\rho}$ (Kinematic Viscosity).

3.3 Solution to the Axial Navier-Stokes

From the axial Navier-Stokes in equation (13), we consider the initial and boundary conditions, which is given as follows:

$$u_z(r, 0) = 0 \text{ (Initial condition)}$$

$$u_z(0, t) \in \mathbb{R} \text{ (Finite velocity along the axis and bounded)}$$

$$u_z(R, t) = 0 \text{ (No-slip condition)}$$

For convenience, we introduce the following dimensionless quantities.

$$u = \frac{U - u_z}{U}$$

$$\eta = \frac{r}{R}$$

$$\tau = \frac{\nu t}{R^2}$$

Thus the differential equation (13) can be written in dimensionless quantities as follows:

$$-\frac{\nu U}{R^2} \frac{\partial u}{\partial \tau} = -\frac{\nu U}{R^2} \left[\frac{\partial^2 u_z}{\partial \theta^2} + \frac{1}{\eta} \frac{\partial u}{\partial \eta} \right]$$

$$\frac{\partial u}{\partial \tau} = \frac{\partial^2 u_z}{\partial \theta^2} + \frac{1}{\eta} \frac{\partial u}{\partial \eta} \tag{14}$$

And the corresponding dimensionless initial and boundary conditions are:

$$\left. \begin{aligned} u(\eta, 0) &= 1 \text{ (Initial condition)} \\ u(0, \tau) &\text{ is bounded} \\ u(1, \tau) &= 0 \text{ (No - slip condition)} \end{aligned} \right\} \quad (15)$$

Which are now homogenous.

3.4 The Method of Separation of Variables

Although the problem defined by (14) and (15) is time dependent, it is linear in " u " and confined to the bounded spatial domain, $0 \leq \eta \leq 1$. Which makes it easier to be solved by the method of separation of variables.

We begin with the hypothesis that a solution of (14) exists in the separable form and hence it follows that:

$$u(\eta, \tau) = F(\eta)G(\tau) \quad (16)$$

Substituting expression (16) into equation (14) to obtain

$$F \frac{dG}{d\tau} = G \frac{d^2 F}{d\eta^2} + \frac{G}{F} \frac{dF}{d\eta}$$

As G depends only on τ and F only on η , by separation of variables the following ODEs for G and F results:

$$\frac{1}{G} \frac{dG}{d\tau} = -\lambda^2 \quad (17)$$

$$\frac{1}{F} \frac{d^2 F}{d\eta^2} + \frac{1}{F} \frac{1}{\eta} \frac{dF}{d\eta} = -\lambda^2 \quad (18)$$

The choice of a negative constant λ^2 is due to the fact that the solution will decay to zero as time increases, i.e. $u \rightarrow 0$ as $\tau \rightarrow \infty$.

By integration the solution of equation (16) can be derived i.e.

$$\int \frac{dG}{G} = -\lambda^2 \int d\tau$$

$$\ln G = -\lambda^2 \tau$$

$$G = C_0 e^{-\lambda^2 \tau} \quad (19)$$

Where C_0 is integration constant to be determine

In order to determine the solution of the DE (18) for $F(\eta)$ can be written as follows:

$$\frac{d^2 F}{d\eta^2} + \frac{1}{\eta} \frac{dF}{d\eta} + \lambda^2 F = 0$$

Multiplying through by η^2 , we have:

$$\eta^2 \frac{d^2 F}{d\eta^2} + \eta \frac{dF}{d\eta} + \lambda^2 \eta^2 F = 0 \quad (19a)$$

Or, on introducing a change of independent variables,

$$y = \lambda \eta$$

Then we have,

$$\eta = y/\lambda \text{ And } \eta^2 = y^2/\lambda^2 \quad (19b)$$

$$\text{Differentiating } \eta = y/\lambda \quad (19c)$$

$$\frac{d\eta}{dy} = \frac{1}{\lambda}$$

$$\lambda d\eta = dy \implies \lambda d^2 \eta = dy^2$$

$$\Rightarrow d^2\eta = \frac{dy^2}{\lambda} \quad (19d)$$

Putting (19c) and (19d) in to (19a) we have:

$$\frac{y^2}{\lambda^2} \left[\frac{d^2F}{dy^2} \cdot \lambda \right] + y/\lambda \left[\frac{dF}{dy} \cdot \lambda \right] + \lambda^2 \cdot \frac{y^2}{\lambda^2} F = 0$$

$$\frac{y^2}{\lambda} \left[\frac{d^2F}{dy^2} \right] + y \left[\frac{dF}{dy} \right] + y^2 F = 0$$

Since, λ is the constant of separation (i.e. the separation parameter). We assume that λ is unity for convenience purpose we obtain:

$$y^2 \frac{d^2F}{dy^2} + y \frac{dF}{dy} + y^2 F = 0$$

$$y^2 F'' + y F' + y^2 F = 0 \quad (20)$$

Hence, equation (20) is the Bessel differential equation of order zero (0).

3.5 Solution of the Bessel Differential Equation

From equation (20) Bessel differential equation of order zero; by applying the generalized power series (i.e. Frobenius Method) to obtain the two independent solutions

$$LF = y^2 F'' + y F' + y^2 F = 0 \quad (21)$$

Let:

$$\left. \begin{aligned} F &= \sum_{n=0}^{\infty} a_n y^{n+r} \\ F' &= \sum_{n=0}^{\infty} (n+r) a_n y^{n+r-1} \\ F'' &= \sum_{n=0}^{\infty} (n+r)(n+r-1) a_n y^{n+r-2} \end{aligned} \right\} \quad (22)$$

$$LF = \sum_{n=0}^{\infty} a_n [(n+r)(n+r-1) + (n+r)] y^{n+r} + a_n y^{n+r+2} = 0 \quad (23)$$

$$m = n + 2, n = m - 2$$

$$0 = \sum_{n=2}^{\infty} a_n [(n+r)^2 + a_{n-2}] y^{n+r} + a_0 [r(r-1) + r] y^r + a_1 [r(r-1) + r + 1] y^{r+1} = 0 \quad (24)$$

The indicial equation is:

$$a_0 r^0 = 0 \quad r_{1,2} = 0, 0 \quad (\text{a double root})$$

$$r_1 = 0 \Rightarrow a_1 \cdot 1 = 0 \Rightarrow a_1 = 0$$

RECURSION:

$$a_n = -\frac{a_{n-2}}{(n+r)^2} \quad n \geq 2$$

$$\left. \begin{aligned} a_2 &= -\frac{a_0}{2^2}; \\ a_4 &= -\frac{a_2}{4^2} = \frac{a_0}{2^2 4^2}; \\ a_6 &= -\frac{a_4}{6^2} = -\frac{a_0}{2^2 4^2 6^2}; \\ a_8 &= -\frac{a_6}{8^2} = \frac{a_0}{2^2 4^2 6^2 8^2}; \\ &\vdots \\ &\vdots \\ &\vdots \end{aligned} \right\} \quad (25)$$

$$a_{2m} = \frac{(-1)^m}{2^{2m} (m!)^2} a_0 \quad (26a)$$

$$F_1(y) = \left[1 + \sum_{m=1}^{\infty} \frac{(-1)^m y^{2m}}{2^{2m} (m!)^2} a_0 \right] = J_0(y) \quad (26b)$$

To get the second solution:

$$F(y, r) = a_0 y^r \left[1 - \frac{y^2}{(2+r)^2} + \frac{y^4}{(2+r)^2 (4+r)^2} + \cdots + \frac{(-1)^m y^{2m}}{(2+r)^2 (4+r)^2 \cdots (2m+r)^2} + \cdots \right] \quad (27)$$

$$\begin{aligned} \frac{\partial F}{\partial r}(y, r) \Big|_{r=r_1} &= a_0 \log_y F_1(y) \\ &+ a_0 y^r \sum_{m=1}^{\infty} (-1)^m y^{2m} \frac{\partial}{\partial r} \left[\frac{1}{(2+r)^2 \dots (2m+r)^2} \right] \end{aligned}$$

$$\text{Let } a_{2m}(r) = \{ \} \Rightarrow \ln a_{2m}(r) = -2\ln(2+r) - \dots - 2\ln(2m+r) \quad (28)$$

$$\begin{aligned} a'_{2m}(0) &= \left(\frac{-2}{2+r} - \frac{-2}{4+r} - \dots - \frac{-2}{(2m+r)} \right) \Big|_{r=0} a_{2m}(0) \\ &= \left(-1 - \frac{1}{2} - \dots - \frac{1}{m} \right) a_{2m}(0) \\ &= H_m a_{2m}(0) \end{aligned}$$

$$\text{Let } H_m = 1 + \frac{1}{2} + \dots + \frac{1}{m} \text{ Therefore,}$$

$$F_1(y) = J_0(y) \ln y + \sum_{m=0}^{\infty} \frac{(-1)^{m+1} H_m}{2^{2m} (m!)^2} y^{2m}, \quad y > 0 \quad (29)$$

It is conventional to define

$$Y_0(y) = \frac{2}{\pi} [f_2(y) + (\gamma - \log 2) J_0(y)] \quad (30)$$

Where

$$\gamma = \lim_{n \rightarrow \infty} (H_n - \log n) = 0.5772 \quad (\text{Euler's constant})$$

$$F(y) = C_1 J_0(y) + C_2 Y_0(y) \quad (31)$$

Thus, equation (31) is the most general solution of equation (20).

A plot showing the behavior of these two functions is shown in figure (3.2)

below. Both oscillate

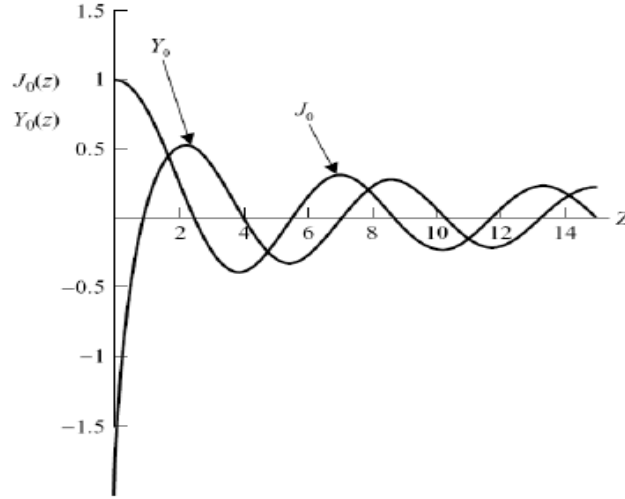


Figure 3.2: Zero order Bessel functions $J_0(z)$ and $Y_0(z)$.

Substituting equation (19) and (31) into (16), we obtain the general solution of the form:

$$u(y, \tau) = e^{-\lambda^2 \tau} [C_1 J_0(y) + C_2 Y_0(y)] \quad (32)$$

We note that the constant C_0 has been dropped since it is redundant here. The solution is bounded at $y = 0$, this condition is satisfied only when the constant $C_2 = 0$.

Hence, the general solution (32) (that is bounded at $y = 0$) takes a form:

$$u(y, \tau) = C_1 J_0(y) e^{-\lambda^2 \tau} \quad (33)$$

We recall that $y = \lambda \eta$

Equation (33) can be written as:

$$u_n(\eta, \tau) = A_n J_0(\lambda_n \eta) e^{-\lambda^2 \tau} \quad (34)$$

3.6 Axial Velocity through the Pipe

From (34) the subscript "n" is added in anticipation of the fact that there is an infinite, but discrete set of values possible for λ such that the general solution (33) satisfies the boundary condition.

$$u = 0 \text{ at } \eta = 1$$

This set of values of $\lambda = \lambda_n$ is known as the eigen values of the problem and the corresponding u_n are called the eigen functions.

To obtain the eigen values λ_n , we apply the boundary condition at $\eta = 1$ to (34), that is:

$$0 = A_n J_0(\lambda_n \eta) e^{-\lambda^2 \tau} \quad \text{for all } \tau$$

Since setting $A_n = 0$ would results in a trivial solution. We say:

$$J_0(\lambda_n) = 0 \tag{35}$$

For the non-trivial solution

Therefore, one obtains multiple values of λ_n (eigen-values) that satisfy the boundary conditions at the wall clearly these eigen values are equal to the infinite set to zeros of the Bessel function of order zero $J_0(z)$ referring to (figure 3.2).

Considering the linearity of the governing equation and boundary conditions (14) and (15), the complete solution for $u_n(\eta, \tau)$ is obtained by linear super positions.

$$U = \sum_{n=1}^{\infty} u_n(\eta, \tau) = \sum_{n=1}^{\infty} A_n e^{-\lambda^2 \tau} J_0(\lambda_n \eta) \tag{36}$$

Where $A_n =$ (arbitrary constant coefficients)

Equation (36) is called the Fourier-Bessel series. This solution satisfies the differential equation (14) and the boundary condition $[u = 0 \text{ at } \eta = 0]$ for any choice of the constant coefficients A_n .

3.7 Orthogonality of the Bessel Function

The orthogonal properties of the Bessel function of order zero states that:

$$\int_0^1 J_0(\lambda_m \eta) J_0(\lambda_n \eta) \eta d\eta = \begin{cases} \frac{1}{2} J_1^2(\lambda_n), & \text{if } n = m \\ 0, & \text{if } n \neq m \end{cases} \quad (37)$$

Where J_1 is the Bessel function of first kind of order 1, multiplying

$(u(\eta, o) = A_n J_0(\lambda_n \eta) = 1)$ by $\eta J_0(\lambda_m \eta)$ and integrating over η from 0 to 1, we obtain.

$$\sum_{n=1}^{\infty} A_n \int_0^1 J_0(\lambda_m \eta) J_0(\lambda_n \eta) \eta d\eta = \int_0^1 \eta J_0(\lambda_m \eta) d\eta$$

Due to the orthogonality property in (37), the nonzero term on the left hand side is that for $m = n$ hence.

$$A_n = \frac{\int_0^1 \eta J_0(\lambda_n \eta) d\eta}{\int_0^1 \eta J_0^2(\lambda_n \eta) d\eta} = \frac{\int_0^1 \eta J_0(\lambda_n \eta) d\eta}{\frac{1}{2} J_1^2(\lambda_n)} \quad (38)$$

For evaluating the numerator of (38), we use the following Bessel function:

$$\int \eta^{p+1} J_p(J_n) d\eta = \frac{1}{\lambda} \eta^{p+1} J_{p+1}(\lambda \eta)$$

Therefore we also have, $\int_0^1 \eta J_0(\lambda_n \eta) d\eta = \frac{1}{\lambda_n} \eta J_1(\lambda_n \eta)$

And thus, the numerator of equation (38) becomes:

$$\int_0^1 \eta J_0(\lambda_n \eta) d\eta = \frac{1}{\lambda_n} J_1(\lambda_n) \quad (39)$$

Substituting equation (39) into (38) yields an expression for A_n

$$A_n = \frac{\int_0^1 \eta J_0(\lambda_n \eta) d\eta}{\int_0^1 \eta J_0^2(\lambda_n \eta) d\eta} = \frac{\frac{1}{\lambda_n} J_1(\lambda_n)}{\frac{1}{2} J_1^2(\lambda_n)} = \frac{2}{\lambda_n} [J_1(\lambda_n)]^{-1}$$

$$A_n = \frac{2}{\lambda_n} [J_1(\lambda_n)]^{-1} \quad (40)$$

Thus for the velocity distribution according to (36), results:

$$u_n(\eta, \tau) = 2 \sum_{n=1}^{\infty} \frac{1}{\lambda_n J_1(\lambda_n)} e^{-\lambda_n^2 \tau} J_0(\lambda_n \eta) \quad (41)$$

The above Fourier-Bessel series has the property of converging very quickly when the dimensionless time $\left(\tau = vt/R^2\right)$ is large. On the other hand, the convergence is slow when τ is small. Reverting to dimensional variables, we can express the solution of the full, original problem in terms of the axial velocity profile.

$$u_z(r, t) = \left[1 - 2 \sum_{n=1}^{\infty} \frac{1}{\lambda_n J_1(\lambda_n)} e^{-\lambda_n^2 vt/R^2} J_0\left(\lambda_n \frac{r}{R}\right) \right] \quad (42)$$

3.8 Shear Stress Distribution in the Pipe

The shear stress distribution in the flow field can be easily obtained from the velocity distribution as follows:

$$\tau_{rx} = \mu \left(\frac{\partial u_r}{\partial x} + \frac{\partial u_x}{\partial r} \right) = -\mu \frac{du_z}{dr} \quad (43)$$

The negative sign is introduced because in a pipe as the radius $\frac{du_z}{dr}$ increases velocity decreases.

In dimensionless form, we have:

$$\tau_{rx} = \frac{du}{d\eta}$$

Where dimensionless stress $\tau_{rx} = \frac{\tau_{rx}}{\mu u/R}$ for evaluating the derivative of velocity profile we make use of the following property of Bessel function.

$$\frac{d}{d\eta} [\eta^{-p} J_p(\lambda_n)] = -\lambda \eta^{-p} J_{p+1}(\lambda_n) \quad (44)$$

Therefore;

$$\frac{d}{d\eta} [J_0(\lambda_n)] = -\lambda J_1(\lambda_n) \quad (45)$$

And thus the shear stress profile is given by:

$$\tau_{rx} = \frac{du}{d\eta} = -2 \sum_{n=1}^{\infty} [J_1(\lambda_n)]^{-1} e^{-\lambda_n^2 \tau} J_1(\lambda_n \eta)$$

For the value of wall stress at the pipe wall, i.e. at $\eta = 1$, one obtains

$$\tau_{wall} = \left. \frac{du_z}{dr} \right|_{r=R} = -\frac{2\mu u}{R} \sum_{n=1}^{\infty} e^{-\lambda_n^2 \tau} \quad (46)$$

It can be seen that the wall shear stress has a finite value, even for time $t = 0$ this is a surprising result when comparing to other cases where flow is induced by impulsively motion of the boundary. Note also that the wall shear stress $\tau_{wall} \rightarrow 0$ at $t \rightarrow \infty$.

CHAPTER FOUR

RESULTS, DISCUSSION AND CONCLUSION

4.0 Introduction

In this chapter, we used the solutions of Bessel of order zero, velocity profile and shear stress gotten in chapter three to obtain the appropriate graphical illustrations of the equations: (26), (30), (31), (42) and (46) subject to the appropriate boundary conditions for each of the equations. The results are obtained at several time rate of blood flow, alongside with the required parameters. These results will be discussed and conclusion shall be drawn based on the findings from our results. All the solutions are obtained using MATLAB programming language.

4.1 Results

The results of the study as illustrated graphically are shown below:

S/N	Parameters/ Variables	Meaning	Value	Source
1	t	Time of flow	$t \in [0, 20]$	Estimated
2	ρ	Density of blood	1060 kg/m^3	Wang,(2014)
3	γ	Kinematic viscosity of blood	$274 \text{ mm}^2/\text{s}$	Wang,(2014)
4	r	Inner radius of artery	0.45 cm	Wang,(2014)
5	R	Radius of the artery	0.75 cm	Wang,(2014)
6	η	Dimensionless parameter for boundary conditions	0.6	Estimated $\eta = \frac{r}{R}$
7	ν	Kinematic viscosity	$\frac{m}{v}$	Estimated
8	τ	Shear stress distribution	$\frac{\nu * t}{R^2}$	Estimated

9	λ	The appropriate separation constant.	0.3	Assumed
10	μ	Viscosity	$3.2 * 10^{-2}\text{Pas}$	Tivde, (2012)

Table 4.1 Parameter values for the Model

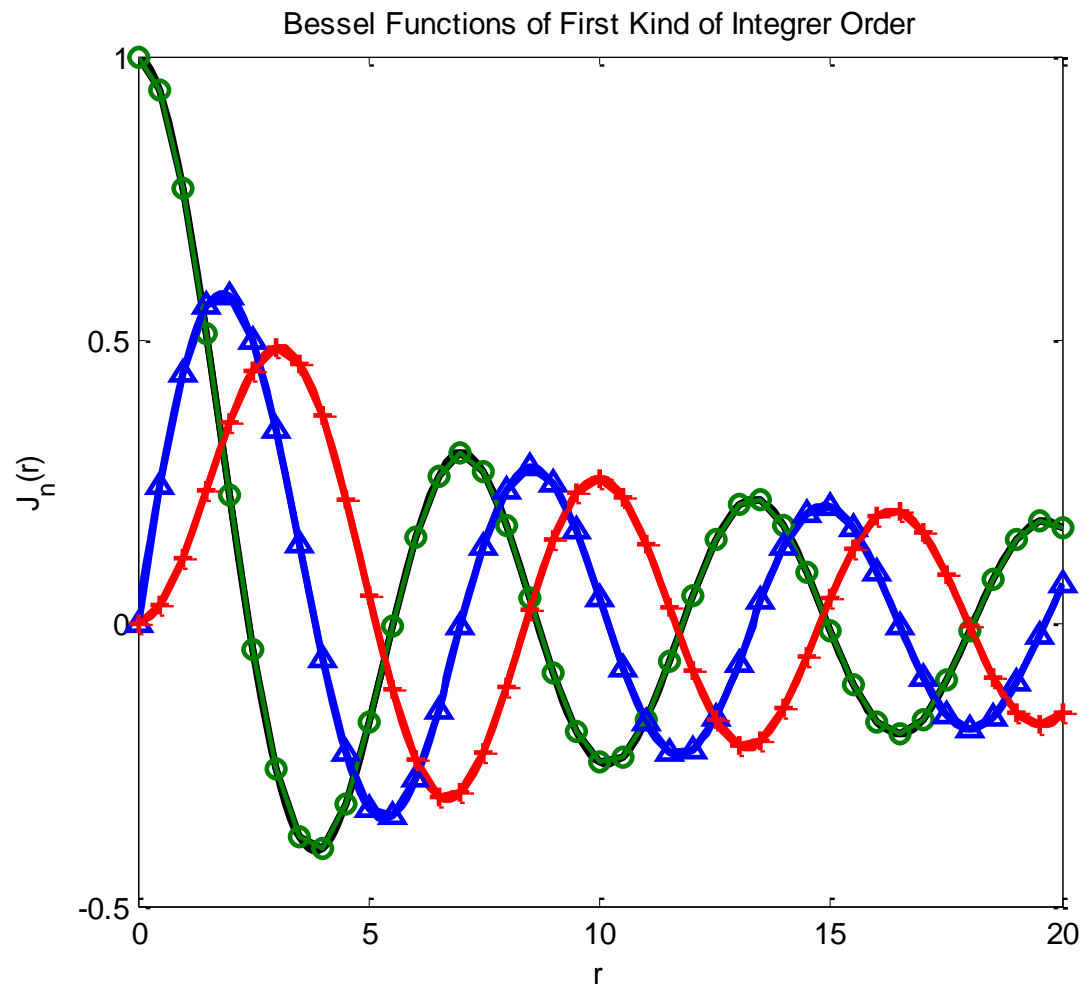


Figure 4.1 Graph showing the behaviour and oscillation of Bessel function of first kind of integer order at J_0, J_1 and J_2 .

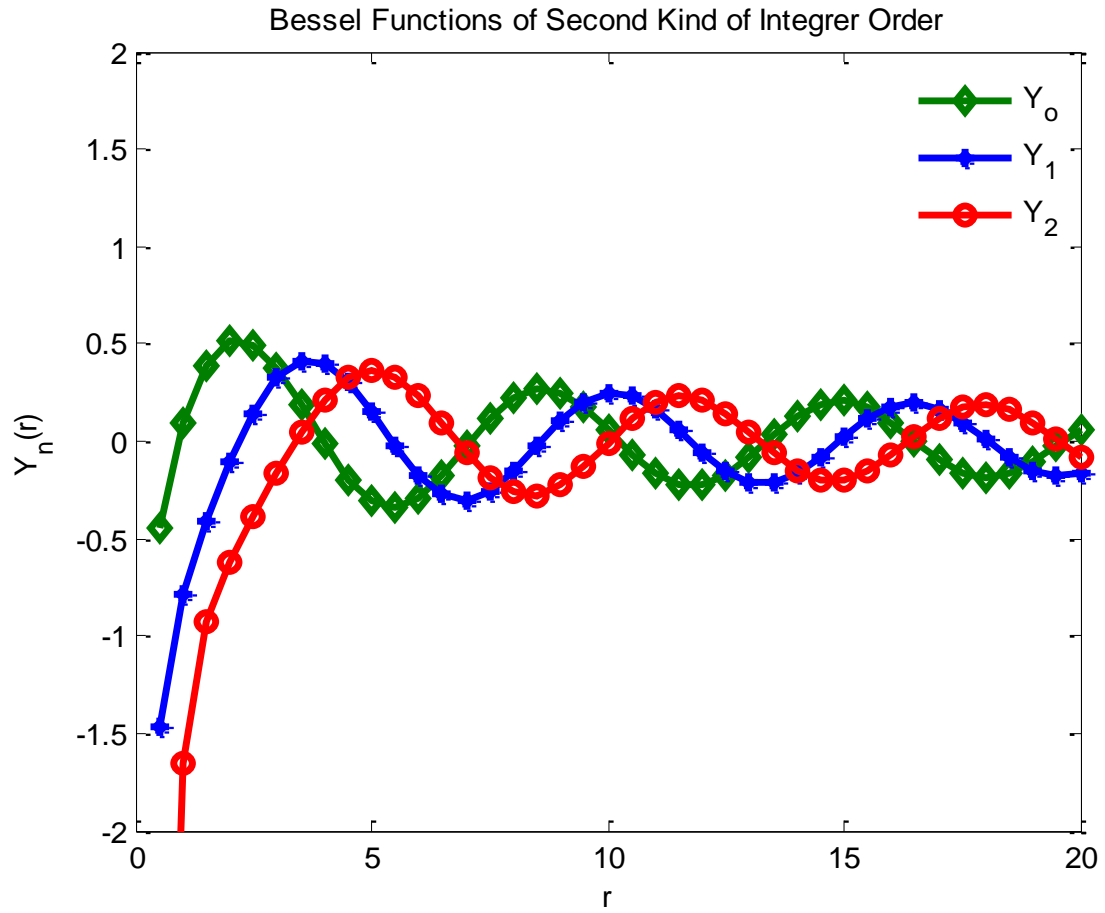


Figure 4.2 Graph showing the behaviour and oscillation of Bessel function of second kind of integer order at Y_0, Y_1 and Y_2 . The ordinary Bessel function Y_n is oscillatory, exhibiting no singularity (appropriate for the field within the core).

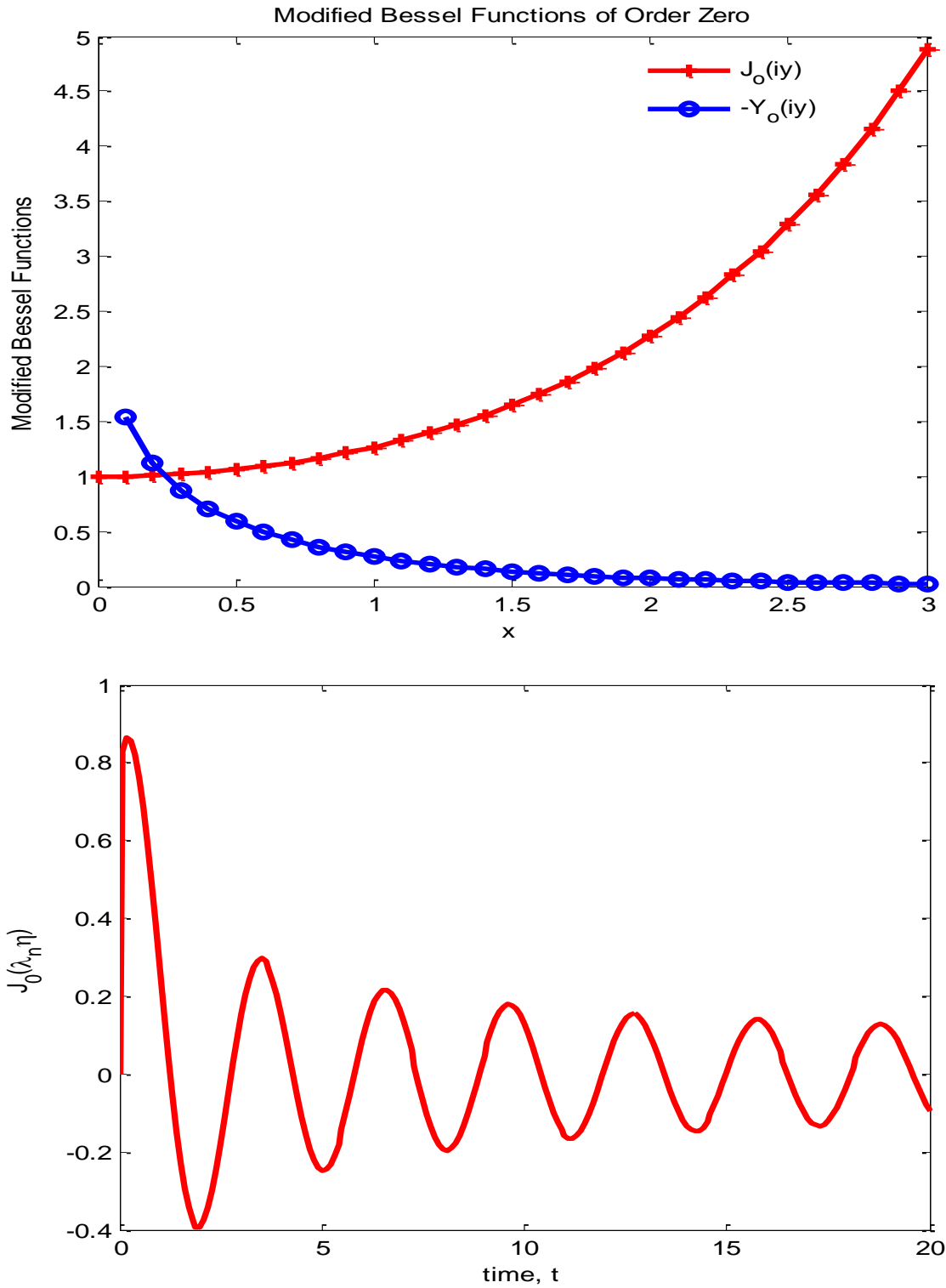


Figure 4.3 Graph showing the behaviour and oscillation of the Modified Bessel function of order zero the modified Bessel function J_0 resembles an exponential decay (appropriate for the field in cladding).

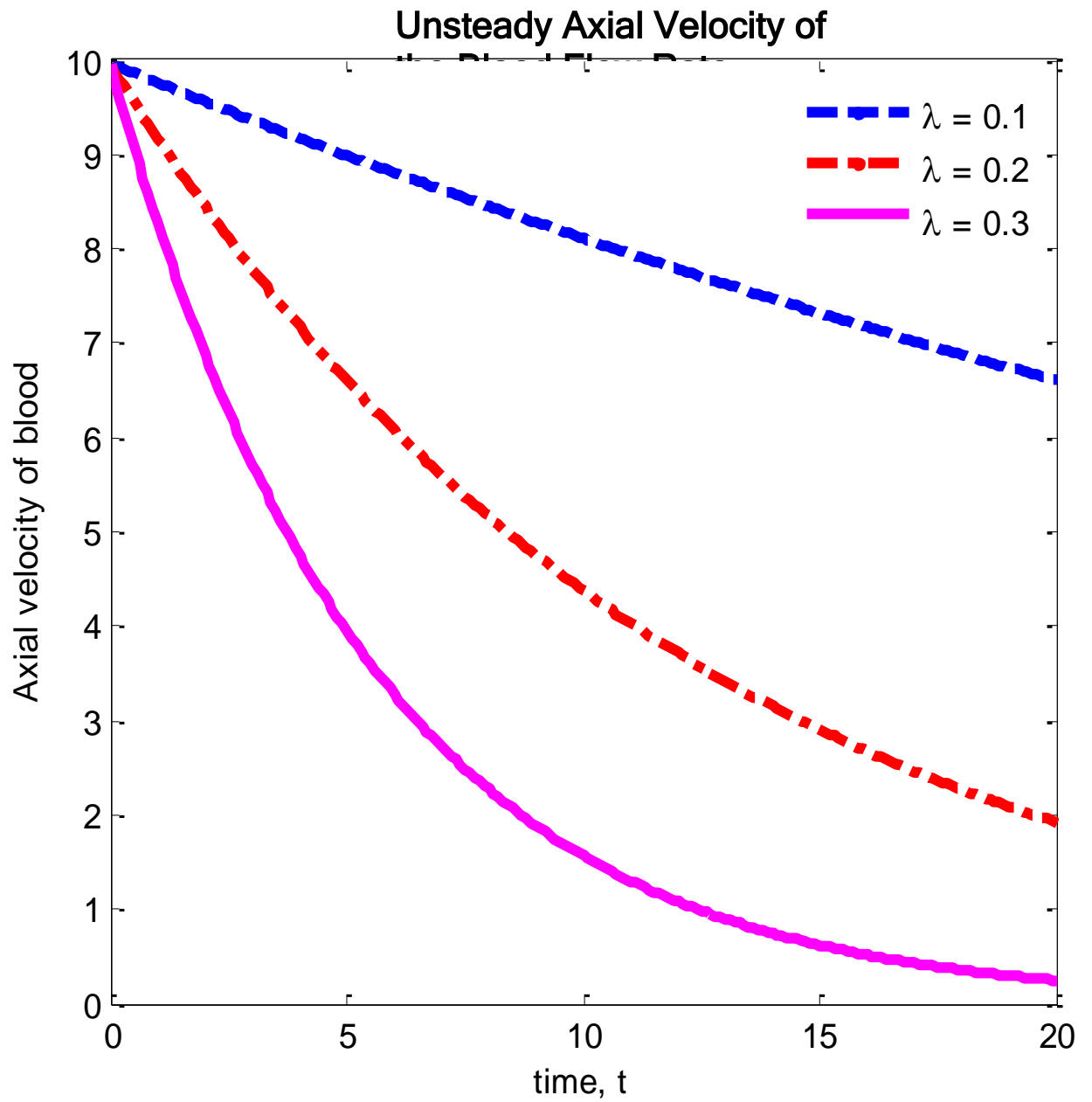


Figure 4.4 Graph showing the Axial Velocity Profile as a Function of axial location at $\lambda_1 = 0.1$, $\lambda_2 = 0.2$ and $\lambda_3 = 0.3$ in respect to the corresponding time of flow within the pipe.

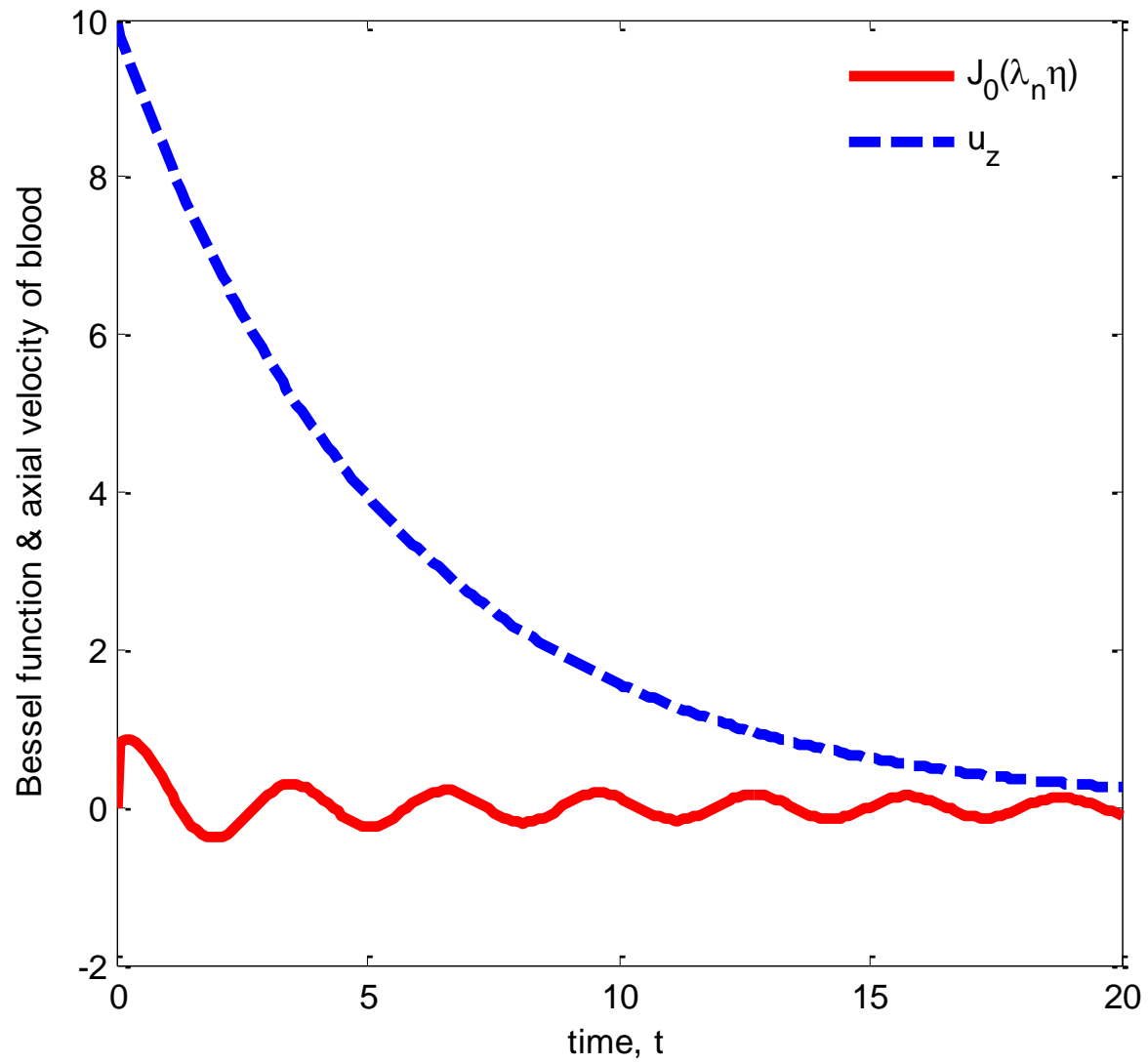


Figure 4.5 Graph showing the relationship between the Bessel function of order zero and the Axial Velocity Profile of blood flow

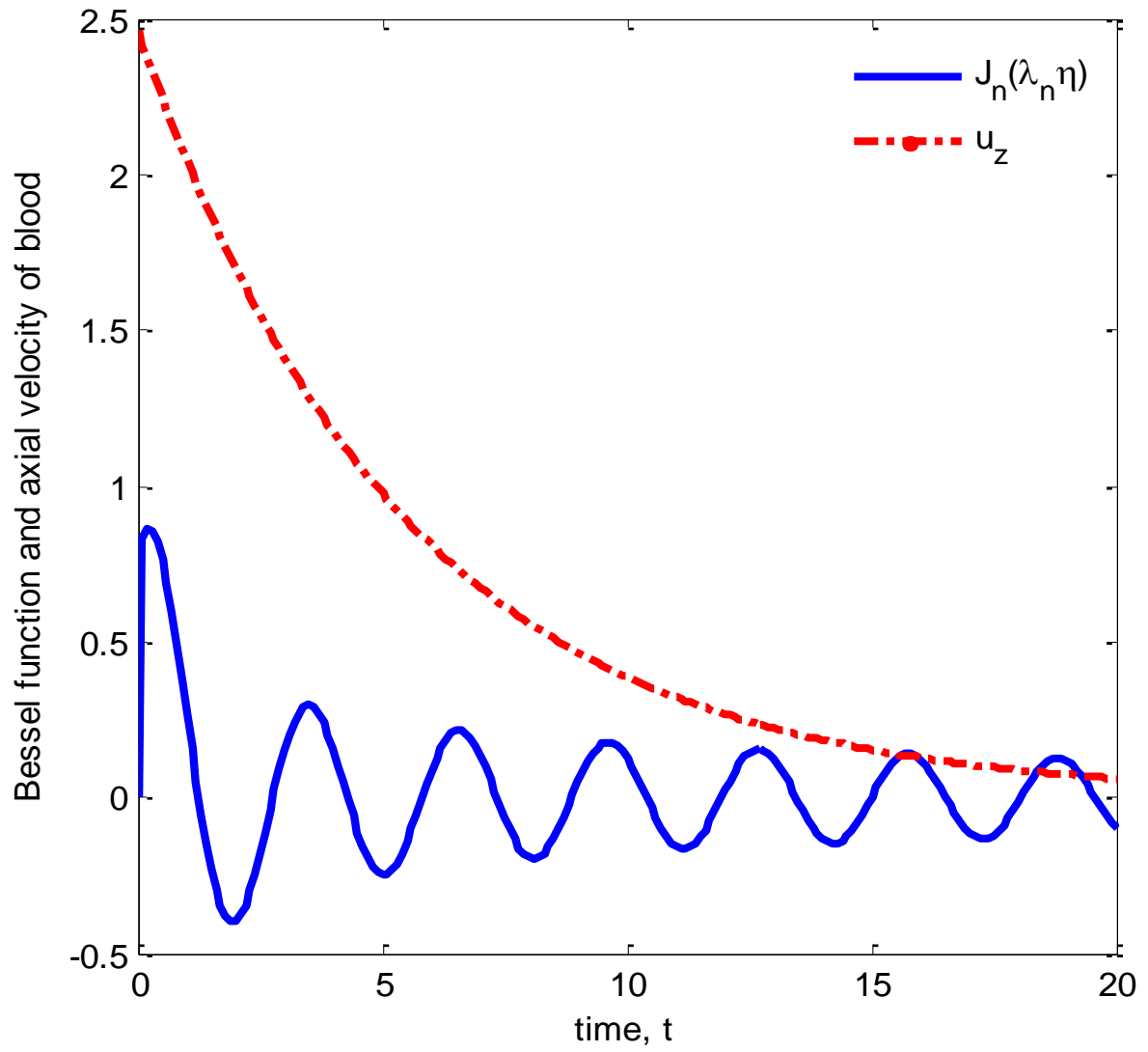


Figure 4.6 Graph showing the relationship between the Bessel function of order n and the Axial Velocity Profile of blood flow

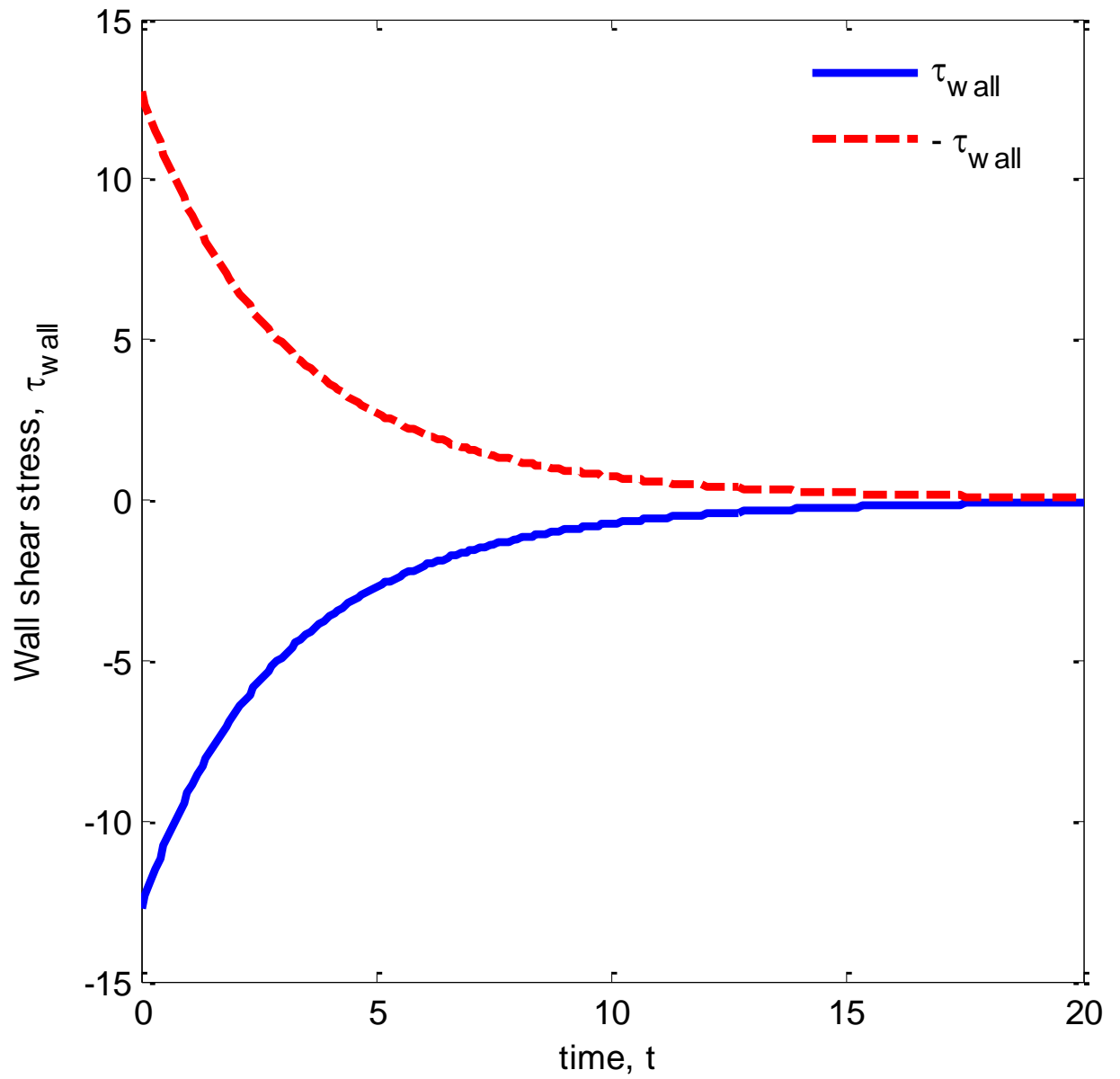


Figure 4.7 Graph showing the shear stress distribution in the flow field as specific interval of time flow rate ranging from $t = 0$ and as $t \rightarrow \infty$ within the pipe.

4.2 Discussion

We shall discuss in details the fluid characteristics of the axial velocity profile graph represented in Figure 4.4 and the shear stress distribution in the flow from Figure 4.7.

4.2.1 Discussion on the Axial Velocity Profile Graph in Figure 4.4

Considering the incompressible fluid flow along a pipe, the boundary layer places a major effect on the fluid characteristics. At the initial boundary condition $u_z(r, 0) = 0$ the fluid will experience a free stream; in which the boundary layer starts growing because the fluid elements close to the wall will feel the effect of the wall strongest since the wall brought the fluid to rest at that point and because of the viscosity the effect is propagated to the outer plane. And those fluids from the wall will feel some effect of the wall but not that strong because they are also pulled by the fluid elements on the opposite side which is moving faster. The farther you go from the wall i.e. $u_z(R, t) = 0$ we discovered that those fluid elements will feel no effect at all yielding to No-slip condition. Hence, we see that viscosity is not capable of creating farther velocity gradient.

From equation (42) which represents our unsteady axial velocity profile as shown in Figure 4.4, plotting λ (viscosity) against the time of flow (t) we observed that the velocity maintains a uniform state as it approaches a fixed point and u_z (*axial velocity*) experiences vanishing at the round boundary, and all the declining profiles, whose maximum is gradually reduced with time, until complete extinction.

The result agrees with the work of Womersley (1955) on the stability of poiseuille flow and its uniform velocity. However, Womersley work is limited to modeling laminar flow through a rigid tube. As u_z converges perfectly to zero at the boundary layer. Our result is confirmed also via the work of Brenn (2017). In which he considered the linearization for cylindrical flow solved using Legendre function of first and second kind.

4.2.2 Discussion on the Shear Stress Distribution Graph in Fig.4.7

Any real fluid moving along solid boundary will undergo a shear stress exerted on that boundary. The No-slip condition dictates that the velocity of the fluid relative to the boundary is zero; but, at some height from the boundary the flow velocity must equate that of the unperturbed fluid. The region between these two points is aptly named the boundary layer for all Newtonian fluids in laminar flow the shear stress is proportional to the strain rate in the fluid, the viscosity being the constant of proportionality. Using the velocity field, we derived the shear stress as expected, which is determined only by the transient component of the velocity $u_z(r, t)$ in (42). By focusing on a particular instant of time, we obtained the law of the shear stress in the fluid at different radial r values. Repeating the process for several instances of time we observed that:

- first for $t = 0$, such as physics suggest that $\tau_{wall} \rightarrow 0$. But we see that the wall shear stress has a finite value. This is a surprising result when comparing to other cases where flow is induced by impulsively motion of the boundary.
- then, we observed that as the time t increases the pseudo-oscillation decays gradually until it turns to zero. That is, to say, that the wall

shear stress $\tau_{wall} \rightarrow 0$ at $t \rightarrow \infty$. Hence, the family of the stress profile is dying and drives to equilibrium.

4.3 Conclusion

The detection of Navier-Stokes analytical unsteady solutions has been rather trendy for the last 200 years, such that a (non-exhaustive) outline of the most recent literatures (books and papers) has been provided in our work. Each of these possible solutions requires some physical assumptions for passing to a tractable PDE system: our basic ones are that the pressure axial gradient keeps itself on its hydrostatic value and no radial velocity arises (strictly considering the axial velocity). We provided an integration of a polar coordinate Navier-Stokes equation system for an unsteady state laminar flow of incompressible fluid in a cylinder spinning about its axis considering only the axial plane as illustrated in figure 3.1. The axial problem PDE (13), (14) has been solved under condition (15); so that the relevant solution is given by formular (42), plotted at figure 4.4. The shear stress is then computed using the velocity field given in (42) resulting to (46).

Finally, we deduced that our analytical solution model has shown that past numerical and analytical treatment of non-Newtonian fluid application have inaccurate velocity profiles; from results of Duggins (1972) as clearly stated in the work of Stephen (1995). The concern with the past model is that the region of extreme error is in the time dependent portion of the solutions, since most where approach using numerical approaches. The velocity and shear stress profiles predicted in the closed form solution presented here will provide the accuracy needed to analyze flows with small time durations that include impulse loads, such as the oscillating flow of blood in an artery.

REFERENCES

- Alessio, B., Giovanni, M. S. and Daniele, R. (2016). Unsteady Rotating Laminar Flow: Analytical solution of Navier-Stokes Equations. *Journal of Fluid Dynamics*. arXiv:1609.05392[physics.flu.dyn]. Vol.2, 2-6.
- Antonova, N., Tosheva, N. and Velcheva, P. (2012). Numerical analysis of blood flow and common carotid artery hemodynamics in the carotid artery bifurcation with stenosis. *Series on Biomechanics*. 27(3-4), 5-10.
- Atlas, G.M. and Desilverio, M.C. (2006). *Solutions to the Van der Pol Equation: a Model of Aortic Blood Flow*. Conference: Bioengineering Conference. Proceedings of the IEEE 32nd Annual Northeast, 2006.
- Brenn, G. (2017) *Analytical Solutions for Transport Processes: Fluid Mechanics, Heat Mass Transfer*. Berlin: SpringerLinks. <http://dx.doi.org/10.1007/978-3-662-51423-8>.
- Boyce, E. and Prima, D. (2015). *The One Dimensional Wave Equation: D'Alembert's Solution*. Introduction to lecture note on PDE University of Washington, 2015.
- David, F. M., Gheona, A., Randall, P., Julio. A. P., Emilios, D. and Raphael, S. (2002). Arterial Wall Properties and Womersley Flow in Fabry Disease. *Journal of BioMed Central*, 2(1): 1471-2261.
- Dennis, G. Z. and Warren, S. (2012). *Differential Equations with Boundary-value Problems, Eighth Edition*. USA: Thomson Brooks. ISBN 10:0534380026/ISBN 13:9780 5343 80021.
- Dochan, K. (1984). An Incompressible Navier-Stokes Flow Solver in Three-Dimensional Curvilinear Coordinate Systems Using Primitive Variables. *AIAA 22nd Aerospace Science Meeting*. January 9-12, 1984/Reno, Nevada.
- Drazin, P. and Riley, N. (2006). *The Navier-Stokes equations: a classification of flows and Exact Solutions*. London: Cambridge University Press.
- Euler, L. (1757). Principes généraux du mouvement des fluides, Mémoires de l'Acad. *Journal of Des Sciences de Berlin*. 11(1): 274-315.
- Gabriella, S. (2011). *Numerical Solution of Two-point Boundary Value Problems*. Budapest, Hungary; B.sc Thesis Department of Applied Analysis and Computational Mathematics, Eotvos Lorand University; 2011.
- Hunter P.J. (1972) *Numerical Solution of Arterial Blood Flow*. Auckland, New Zealand; M.sc Thesis, University of Auckland; 1972.
- Huo Y, and Kassab G.S. (2006) Pulsatile Blood Flow in the Entire Coronary Arterial Tree: Theory and Experiment. *Am J Physiol Heart Circ Physiol* 2006, 291(3):H1074-87.

- Jennifer, N. (2008). *Bessel functions and their Applications*. university of Tennessee, 2008.
- John, M. C. and Yunus, A. (2014). *Fluid mechanics: fundamental and Applications*. New York: McGraw-Hill Companies.322-377.
- Joseph, H. S. and Nuri, A. (2008). *Fluid Mechanics, Second Edition*. Berlin, Germany: Springer publish. ISBN 978-3540-73536-6.
- Knyazev, D. V. (2011). Axisymmetric flows of an incompressible fluid between movable rotating disks. *Journals of Fluid Dynamics*. 46 (4):558-564.
- Mabotuwana,T., Cheng, L. K. and Pullan, A. J. (2007). A model of blood flow in the mesenteric arterial system. *BioMedical Engineering OnLine* 2007, 6:17.
- Marmanis H., Hammon C. W. and Kirby R. M. (2006). A one-Dimensional Model of the Navier-Stokes. *Sci Institute Technical Report*. USA; 2006.
- McMahon, J. (1894). On the roots of the Bessel and certain related functions. *The Annals of Mathematics*. 9(1/6): 23-30.
- Salih, A. (2011). *An Exact Solution of Navier–Stokes Equation*. Research work; Department of Aerospace Engineering, Indian Institute of Space Science and Technology. Kerala, India; July 2011.
- Shapiro, A. (2006). An analytical solution of the Navier-Stokes equations for unsteady backward stagnation-point flow with injection or suction. *Journal of Applied Mathematics and Mechanics*. 86(4): 281-290.
- Stephen, A. A. (1995). An Analytical Solution for the Unsteady Flow of a Bingham Plastic Fluid in a Circular Tube. *Research of the Naval Undersea Warfare Centre (NUWC)*. NewLondon (code 2121), TR11,011; 1-16.
- Tivde, T. (2012). *Mathematical modeling of Blood flow in the Internal Carotid Artery*. LAP LAMBERT Academic publishing GmhH & Co. KG 978-3-659-13738-9.
- Tong, L. and Suncica, C. (2009). Critical threshold in a quasilinear Hyperbolic Model of Blood Flow. *Journal of Mathematical Sciences*. 4(65): 527-536.
- Vergara, C., Ponzini, R., Alessandro, V., Alberto, R., Danilo, N. and Oberdan, P. (2010). Womersley number-based estimation of flow rate with Doppler ultrasound: sensitivity analysis and first clinical application. *Computer Methods and Programs in Biomedicine*, 98(2): 151-160.
- Vivian, M. (2011). *History of the circulatory system: discovery of the basics*. Reviewed work of Adam Garber, Medicine 2010 and Michael Livingston, Medicine 2011.

- Vladimir, Z. (2009). *Bessel functions and their Applications to solutions of Partial Differential Equations*. Lecture note of University of Arizona, USA; 2011.
- Vlachakis, N., Fatsis, A., Panoutsopoulou, A., Kouskouti, M. and Vlachakis, V. (2006). An Exact Solution of the Navier-Stokes Equations for Swirl flow models through Porous pipes. *Journals in Advance Fluid Mechanics*. Vol.52, ISSN 1743-3533(on-line), 583-591.
- Wang, X. (2014). 1D Modeling of Blood flow in Networks: numerical computing and applications. *Mechanics [physics]*. Universite Pierre et Marie Curie-Paris VI, 2014; English.
- Wormersley, J. R. (1955). Method for the Calculation of Velocity, Rate of Flow and Viscous Drag in Arteries when the Pressure Gradient is known. *Department of physiology, St Bartholomew's Hospital medical college*. London, 127:553-563.
- Zamm, Z. and Angew,s. (2006). An analytical solutions of the Navier-Stokes equations for unsteady backward stagnation-point flow with injection or suction. *Journal of Applied Mathematics and Mechanics*, (86)4:281–290.